Light Higgses at the Tevatron and at the LHC and Observable Dark Matter in SUGRA and D-branes

Daniel Feldman[1], Zuowei Liu[2] and Pran Nath[3]

Department of Physics, Northeastern University, Boston, MA 02115, USA

Abstract

Sparticle landscapes in mSUGRA, in SUGRA models with nonuniversalities (NUSUGRA), and in D-brane models are analyzed. The analysis exhibits the existence of Higgs Mass Patterns (HPs) (for $\mu > 0$) where the CP odd Higgs could be the next heavier particle beyond the LSP and sometimes even lighter than the LSP. It is shown that the Higgs production cross sections from the HPs are typically the largest enhancing the prospects for their detection at the LHC. Indeed it is seen that the recent Higgs production limits from CDF/DØ are beginning to put constraints on the HPs. It is also seen that the $B_s \to \mu^+\mu^-$ limits constrain the HPs more stringently. Predictions of the Higgs production cross sections for these patterns at the LHC are made. We compute the neutralino-proton cross sections $\sigma(\tilde{\chi}_1^0 p)$ for dark matter experiments and show that the largest $\sigma(\tilde{\chi}_1^0 p)$ also arise from the HPs and further that the HPs and some of the other patterns are beginning to be constrained by the most recent data from CDMS and from Xenon10 experiments. Finally, it is shown that the prospects are bright for the discovery of dark matter with $\sigma(\tilde{\chi}_1^0 p)$ in the range $10^{-44\pm.5}$cm^2 due to a "Wall" consisting of a copious number of parameter points in the Chargino Patterns (CPs) where the chargino is the NLSP. The Wall, which appears in all models considered (mSUGRA, NUSUGRA and D-branes) and runs up to about a TeV in LSP mass, significantly enhances the chances for the observation of dark matter by SuperCDMS, ZEPLIN-MAX, or LUX experiments which are expected to achieve a sensitivity of 10^{-45} cm^2 or more.

Recently a new approach for the search for sparticles at colliders was given in the framework of sparticle landscapes [1]. In this work it is shown that while in the MSSM, which has 32 sparticles, the sparticle masses can generate as many 10^{28} mass hierarchies, the number of these mass hierarchies decreases enormously in well motivated models such as gravity mediated breaking models [2, 3]. It is further shown that if one limits one self to the first four sparticles aside from the lightest Higgs boson, then the number of such possibilities reduces even further. Specifically within the minimal supergravity grand unified model [2], mSUGRA, which has a parameter space defined by [2, 4] $m_0, m_{1/2}, A_0, \tan\beta$ and the sign of the Higgs mixing parameter μ, one finds that the number of such patterns reduces to 16 for $\mu > 0$, and these patterns are labeled mSP1-mSP16 [1]. These patterns are further classified by the next to the lightest sparticles beyond the LSP which are found to be the chargino for mSP$(1-4)$, the stau for mSP$(5-9)$, the stop for mSP$(11-13)$, and the Higgs A/H, where A is the CP odd Higgs in the MSSM and H is the heavier CP even Higgs, for mSP$(14-16)$. Thus the patterns are labeled the Chargino Pattern, the Higgs Pattern etc. Most of these patterns appear to have escaped attention in previous studies because the parameter searches were based on restricted regions of

[1]E-mail: feldman.da@neu.edu
[2]E-mail: liu.zu@neu.edu
[3]E-mail: nath@lepton.neu.edu

the parameter space. In our analysis we have carried out an exhaustive search under naturalness assumptions in exploring the sparticle landscape and the residual parameter space which satisfies the radiative electroweak symmetry breaking (REWSB), the dark matter relic density constraints and the collider constraints from flavor changing neutral currents and sparticle mass limits. The analysis exhibits a much larger set of patterns than previously seen.

In the analysis presented here we consider a larger class of models than discussed in [1]. Specifically we consider mSUGRA models (for recent works on mSUGRA see, e.g., [5]) with both signs of μ as well as SUGRA models with nonuniversalities (NUSUGRA), and D-brane models. The focus of our work will be Higgs Patterns which we collectively call HPs. It will be shown that typically the HPs lead to the largest production cross sections for the CP even and CP odd Higgs at the Tevatron and at the LHC. Further, they also lead to an LSP which has a very substantial Higgsino component. It is also shown that the HPs lead to the largest branching ratio for $B_s \to \mu^+\mu^-$. Finally, we show that the largest spin independent neutralino-proton cross section in dark matter experiments also arises from the HPs and the most recent results from the dark matter experiment are beginning to constrain the HPs, and more generally the dark matter experiments can also serve as a discriminator amongst sparticle mass patterns in the landscape.

We begin by discussing the details of the analysis. For the relic density of the neutralino LSP we impose the WMAP3 constraints [6], $0.0855 < \Omega_{\widetilde{\chi}_1^0} h^2 < 0.1189$ (2σ). As is well known the experimental limits on the FCNC process $b \to s\gamma$ impose severe constraints and we use here the constraints from the Heavy Flavor Averaging Group (HFAG) [7] along with the BABAR, Belle and CLEO experimental results: $\mathcal{B}r(b \to s\gamma) = (355 \pm 24^{+9}_{-10} \pm 3) \times 10^{-6}$. A new estimate of $\mathcal{B}r(\bar{B} \to X_s\gamma)$ at $O(\alpha_s^2)$ gives [8] $\mathcal{B}r(b \to s\gamma) = (3.15 \pm 0.23) \times 10^{-4}$ which moves the previous SM mean value of 3.6×10^{-4} a bit lower. In the analysis we use a 3.5σ error corridor around the HFAG value. The total $\mathcal{B}r(\bar{B} \to X_s\gamma)$ including the sum of SM and SUSY contributions (for the update on SUSY contributions see [9]) are constrained by this corridor. The process $B_s \to \mu^+\mu^-$ can become significant for large $\tan\beta$ since the decay has a $\tan^6\beta$ dependence and thus large $\tan\beta$ could be constrained by the current limit which is $\mathcal{B}r(B_s \to \mu^+\mu^-) < 1.5 \times 10^{-7}$ (90% CL), 2.0×10^{-7} (95% CL) [33]. We note that more recently the CDF and DØ have given limits which are about a factor of 10 more sensitive. We have included these preliminary [10] results in this analysis. Additionally, we also impose the current lower limits on the lightest CP even Higgs boson. For the Standard Model like Higgs boson this limit is ≈ 114.4 GeV [11], while a limit of 108.2 GeV at 95% CL is set on the production of an invisibly decaying Standard Model like Higgs by OPAL [11]. For the MSSM we take the constraint to be $m_h > 100$ GeV. We take the other sparticle mass constraints to be $m_{\widetilde{\chi}_1^\pm} > 104.5$ GeV [12] for the lighter chargino, $m_{\widetilde{t}_1} > 101.5$ GeV, $m_{\widetilde{\tau}_1} > 98.8$ GeV for the lighter stop and the stau [5]. The mSUGRA analysis is based on a large Monte Carlo scan of the parameter space with the soft parameters in the

range $0 < m_0 < 4000$ GeV, $0 < m_{1/2} < 2000$ GeV, $|A_0/m_0| < 10$, $1 < \tan\beta < 60$ and both signs of μ are analyzed. In our analysis we use MicrOMEGAs version 2.0.7 [13] which includes the SuSpect 2.34 package [14] for the analysis of sparticle masses, with $m_b^{\overline{\rm MS}}(m_b) = 4.23$ GeV, m_t(pole) = 170.9 GeV, requiring REWSB at the SUSY scale. We have cross checked with other codes [15, 16, 17, 18, 19, 20, 21] and find agreement up to $\sim O(10\%)$.

In the analysis a scan of 2×10^6 models with Monte Carlo simulation was used for mSUGRA with $\mu > 0$ and a scan of 1×10^6 models for $\mu < 0$. Twenty two 4-sparticle patterns labeled mSP1-mSP22 survive the constraints from the radiative electroweak symmetry breaking, from the relic density constraint, and other collider constraints. mSP1-mSP16 which appear for $\mu > 0$ are defined in [1]. For $\mu < 0$ all of the patterns in $\mu > 0$ case appear except for the cases mSP10, mSP14-mSP16. However, new patterns mSP17-mSP22 appear for $\mu < 0$ and are given below

$$\begin{array}{ll} \text{mSP17}: \widetilde{\chi}_1^0 < \widetilde{\tau}_1 < \widetilde{\chi}_2^0 < \widetilde{\chi}_1^\pm \ ; & \text{mSP18}: \widetilde{\chi}_1^0 < \widetilde{\tau}_1 < \widetilde{l}_R < \widetilde{t}_1 \ ; \\ \text{mSP19}: \widetilde{\chi}_1^0 < \widetilde{\tau}_1 < \widetilde{t}_1 < \widetilde{\chi}_1^\pm \ ; & \text{mSP20}: \widetilde{\chi}_1^0 < \widetilde{t}_1 < \widetilde{\chi}_2^0 < \widetilde{\chi}_1^\pm \ ; \\ \text{mSP21}: \widetilde{\chi}_1^0 < \widetilde{t}_1 < \widetilde{\tau}_1 < \widetilde{\chi}_2^0 \ ; & \text{mSP22}: \widetilde{\chi}_1^0 < \widetilde{\chi}_2^0 < \widetilde{\chi}_1^\pm < \widetilde{g} \ . \end{array} \tag{1}$$

A majority of the patterns discussed in [1] and this analysis do not appear in the Snowmass Benchmarks [22], and in the PostWMAP Benchmarks [23]. Since the HPs are a focus of this analysis, we exhibit these below

$$\begin{array}{ll} (i)\ \text{mSP14}: \widetilde{\chi}_1^0 < A, H < H^\pm \ ; & (ii)\ \text{mSP15}: \widetilde{\chi}_1^0 < A, H < \widetilde{\chi}_1^\pm \ ; \\ (iii)\ \text{mSP16}: \widetilde{\chi}_1^0 < A, H < \widetilde{\tau}_1 \ ; & (iv)\ \text{NUSP12}: \widetilde{\chi}_1^0 < A, H < \widetilde{g} \ , \end{array} \tag{2}$$

where A, H indicates that the two Higgses A and H may sometimes exchange positions in the sparticle mass spectra[4]. The cases (i)-(iii) in Eq.(2) arise for $\mu > 0$ and not for $\mu < 0$, and

HPs	m_0 (GeV)	$m_{1/2}$ (GeV)	A_0 (GeV)	$\tan\beta$	NUH ($\delta_{H_u}, \delta_{H_d}$)	NUq3 ($\delta_{q3}, \delta_{tbR}$)	NUG ($\delta_{M_2}, \delta_{M_3}$)
mSP14	1036	562	500	53.5	(0,0)	(0,0)	(0,0)
mSP14	759	511	2315	31.0	(0.256,-0.499)	(0,0)	(0,0)
mSP14	1223	1200	-111	27.4	(0.557,-0.736)	(0,0)	(0,0)
mSP14	740	620	840	53.1	(0,0)	(-0.553,-0.249)	(0,0)
mSP14	1201	332	-731	55.0	(0,0)	(0,0)	(0.383,0.275)
mSP15	1113	758	1097	51.6	(0,0)	(0,0)	(0,0)
mSP15	900	519	1481	54.8	(0,0)	(0,0)	(-0.352,-0.262)
mSP15	1389	551	-167	59.2	(0,0)	(-0.041,0.916)	(0,0)
mSP16	525	450	641	56.0	(0,0)	(0,0)	(0,0)
mSP16	282	464	67	43.2	(0.912,-0.529)	(0,0)	(0,0)
NUSP12	2413	454	-2490	48.0	(0,0)	(0,0)	(-0.285,-0.848)

Table 1: Benchmarks for HPs for $\mu > 0$ in mSUGRA and in NUSUGRA. The 2nd and the 3rd mSP14 pattern show that the HPs can emerge for moderate values of $\tan\beta$. The Benchmarks are computed with SuSpect 2.34 .

the case (iv) in Eq.(2) arises in an isolated region of the parameter space for $\mu > 0$ in the NUSUGRA case discussed later. The sign of μ is very relevant in the analysis not only because

[4]In fact there are cases where all the Higgses $h, H, A, H^\pm$ lie below $\widetilde{\chi}_1^0$.

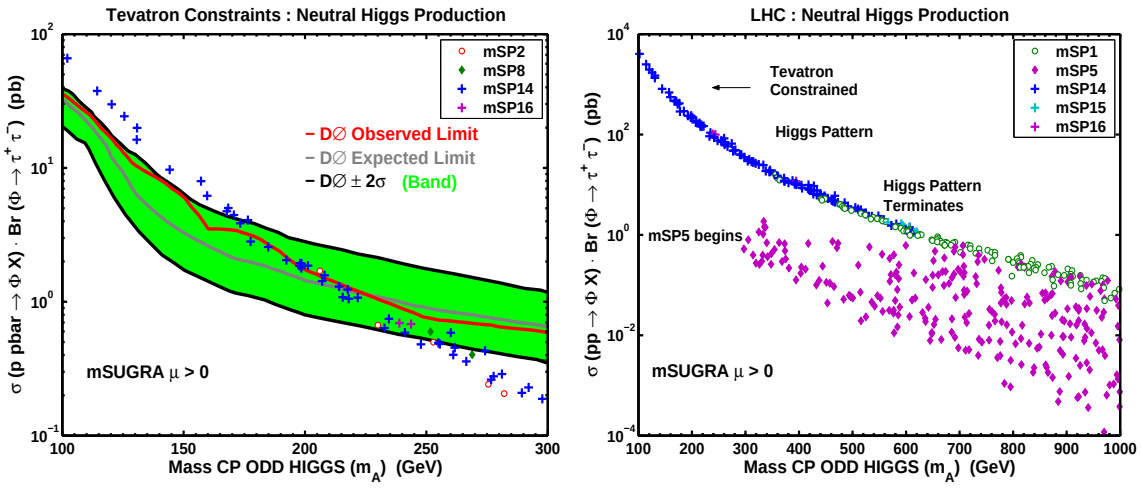

Figure 1: (Color Online) Left panel: Predictions for $[\sigma(p\bar{p} \to \Phi)\mathrm{BR}(\Phi \to 2\tau)]$ in mSUGRA as a function of the CP odd Higgs mass m_A for the HPs at the Tevatron with CM energy of $\sqrt{s} = 1.96$ TeV. The limits from DØ are indicated [27]. Right panel: Predictions for $[\sigma(pp \to \Phi)\mathrm{BR}(\Phi \to 2\tau)]$ in mSUGRA as a function of m_A at the LHC with CM energy of $\sqrt{s} = 14$ TeV for the HPs, the chargino pattern mSP1 and the stau pattern mSP5. The HPs are seen to give the largest cross sections.

the HPs for mSUGRA case arise only for $\mu > 0$, but also because of the recent results from the $g_\mu - 2$ experiment. As is well known the supersymmetric electroweak corrections to $g_\mu - 2$ can be as large or even larger than the Standard Model correction [24]. Further, for large $\tan\beta$ the sign of the supersymmetric correction to $g_\mu - 2$ is correlated with the sign of μ. The current data [25, 26] on $g_\mu - 2$ favors $\mu > 0$ and thus it is of relevance to discuss the possible physics that emerges if indeed one of these patterns is the one that may be realized in nature. Some benchmarks for the HPs are given in Table (1).

Higgs cross sections at the Tevatron and at the LHC: The lightness of A (and also of H and $H^\pm$) in the Higgs Patterns implies that the Higgs production cross sections can be large (for some of the previous analyses where light Higgses appear see [28, 29, 30]). Quite interestingly the recent Tevatron data is beginning to constrain the HPs. This is exhibited in the left panel of Fig.(1) where the leading order (LO) cross section for the sum of neutral Higgs processes $\sigma_{\Phi\tau\tau}(p\bar{p}) = [\sigma(p\bar{p} \to \Phi)\mathrm{BR}(\Phi \to 2\tau)]$ (where sum over the neutral Φ fields is implied) vs the CP odd Higgs mass is plotted for CM energy of $\sqrt{s} = 1.96$ TeV at the Tevatron. One finds that the predictions of $\sigma_{\Phi\tau\tau}(p\bar{p})$ from the HPs are the largest and lie in a narrow band followed by those from the Chargino Pattern mSP2. The recent data from the Tevatron is also shown[27]. A comparison of the theory prediction with data shows that the HPs are being constrained by experiment. Exhibited in the right panel of Fig.(1) is $\sigma_{\Phi\tau\tau}(pp) = [\sigma(pp \to \Phi)\mathrm{BR}(\Phi \to 2\tau)]$ arising from the HPs (and also from other patterns which make a comparable contribution) vs the CP odd Higgs mass with the analysis done at CM energy of $\sqrt{s} = 14$ TeV at the LHC.

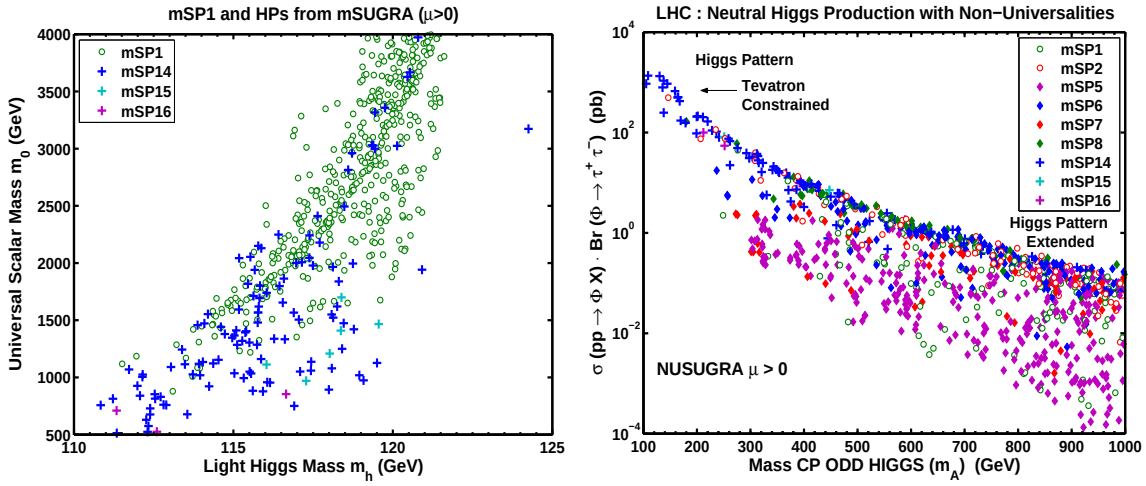

Figure 2: (Color Online) Left panel: mSP1 and HPs are plotted in the m_0-m_h plane in mSUGRA $\mu > 0$. Right panel: Predictions for $[\sigma(pp \to \Phi)\mathrm{BR}(\Phi \to 2\tau)]$ in NUSUGRA (NUH,NUG,NUq3) as a function of CP odd Higgs mass at the LHC showing that the HPs extend beyond 600 GeV with non-universalities (to be compared with the analysis of Fig.(1) under the same naturalness assumptions).

Again it is seen that the predictions of $\sigma_{\Phi\tau\tau}(pp)$ arising from the HPs are the largest and lie in a very narrow band and the next largest predictions for $\sigma_{\Phi\tau\tau}(pp)$ are typically from the Chargino Patterns (CPs). The larger cross sections for the HPs enhance the prospects of their detection. Further, the analysis shows that the Higgs production cross section when combined with the parameter space inputs and other signatures can be used to discriminate amongst mass patterns. Since the largest Higgs production cross sections at the LHC arise from the Higgs Patterns and the Chargino Patterns we exhibit the mass of the light Higgs as a function of m_0 for these two patterns in the left panel of Fig.(2). We note that many of the Chargino Pattern points in this figure appear to have large m_0 indicating that they originate from the Hyperbolic Branch/Focus Point (HB/FP) region[46].

We discuss now briefly the Higgs to $b\bar{b}$ decay at the Tevatron. From the parameter space of mSUGRA that enters in Fig.(1) we can compute the quantity $[(p\bar{p} \to \Phi)\mathrm{BR}(\Phi \to b\bar{b})]$. Experimentally, however, this quantity is difficult to measure because there is a large background to the production from $q\bar{q}, gg \to b\bar{b}$. For this reason one focuses on the production $[(p\bar{p} \to \Phi b)\mathrm{BR}(\Phi \to b\bar{b})]$[47]. For the parameter space of Fig.(1) one gets $[(p\bar{p} \to \Phi b)\mathrm{BR}(\Phi \to b\bar{b})] \lesssim 1$ pb at ($\tan\beta = 55$,$M_A = 200$ GeV). The preliminary CDF data [48] puts limits at 200 GeV, in the range (5-20) pb over a 2σ band at the tail of the data set. These limits are larger, and thus less stringent, than what one gets from $\Phi \to \tau^+\tau^-$. For the LHC, we find $[(pp \to \Phi b)\mathrm{BR}(\Phi \to b\bar{b})] \sim 200$ pb for the same model point. A more detailed fit requires a full treatment which is outside the scope of the present analysis.

$B_s \to \mu^+\mu^-$ and the Higgs Patterns: The process $B_s \to \mu^+\mu^-$ is dominated by the neutral Higgs exchange [31] and is enhanced by a factor of $\tan^6\beta$. It is thus reasonable to expect that the HPs will be constrained more severely than other patterns by the $B_s \to \mu^+\mu^-$ experiment, since HP points usually arise from the high $\tan\beta$ region (we note, however, that the nonuniversalities in the Higgs sector (NUH) can also give rise to HPs for moderate values of $\tan\beta$ (see Table(1))). This is supported by a detailed analysis which is given in Fig.(3) where the branching ratio $\mathcal{B}r(B_s \to \mu^+\mu^-)$ is plotted against the CP odd Higgs mass m_A. The upper left (right) hand panel gives the analysis for the case of mSUGRA for $\mu > 0$ ($\mu < 0$) for the Higgs Patterns as well as for several other patterns, and the experimental constraints are also shown. One finds that the constraints are very effective for $\mu > 0$ (but not for $\mu < 0$) constraining a part of the parameter space of the HPs and also some models within the Chargino and the Stau Patterns are constrained (see upper left and lower left panels of Fig.(3)).

From the analysis of Fig.(3), it is observed that the strict imposition of the constraint $\mathcal{B}r(B_s \to \mu^+\mu^-) < 1.5 \times 10^{-7}$ still allows for large $\tan\beta$ in the mSUGRA model. Thus all of the HP model points given in Fig.(3) that satisfy this constraint for the mSUGRA $\mu > 0$ case correspond to $\tan\beta$ in the range of 50 - 55. A similar limit on $\tan\beta$ is also observed for the nonuniversal models. We remark, however, that the HPs are not restricted to large $\tan\beta$ in particular for the case of the NUH model, where two such benchmarks are given in Table(1) for quite moderate values of $\tan\beta$. Here the HP model points in mSP14 for the NUH case in Table(1) have $\mathcal{B}r(B_s \to \mu^+\mu^-) \sim (3.1, 3.8) \times 10^{-9}$ which are significantly lower than what is predicted by the very large $\tan\beta$ case in models with universality and thus these cases are much less constrained by the $\mathcal{B}r(B_s \to \mu^+\mu^-)$ limits.

Dark Matter-Direct Detection: We discuss now the direct detection of dark matter. In Fig.(4) we give an analysis of the scalar neutralino-proton cross section $\sigma(\tilde{\chi}_1^0 p)$ as a function of the LSP mass (complete analytic formulae for the computation of dark matter cross sections can be found in [34] and for a sample of Post-WMAP3 analysis of dark matter see [35, 36]). The upper left panel of Fig.(4) gives the scalar $\sigma(\tilde{\chi}_1^0 p)$ for the mSUGRA parameter space for $\mu > 0$. We note that the Higgs patterns typically give the largest dark matter cross sections (see the upper left and lower left panels of Fig.(4)) and are the first ones to be constrained by experiment. The second largest cross sections arise from the Chargino Patterns which shows an embankment, or Wall, with a copious number of points with cross sections in the range $10^{-44\pm.5}\text{cm}^2$ (see the upper left panel and lower right panel), followed by Stau Patterns (lower left panel), with the Stop Patterns producing the smallest cross sections (upper left and lower right panels). The upper right panel of Fig.(4) gives the scalar cross section $\sigma(\tilde{\chi}_1^0 p)$ for $\mu < 0$ and here one finds that the largest cross sections arise from the CPs which also have a Chargino Wall with cross sections in the range $10^{-44\pm.5}\text{cm}^2$ (upper right panel). The analysis shows that altogether the scalar cross sections lie in an interesting region and would be accessible to dark matter experiments

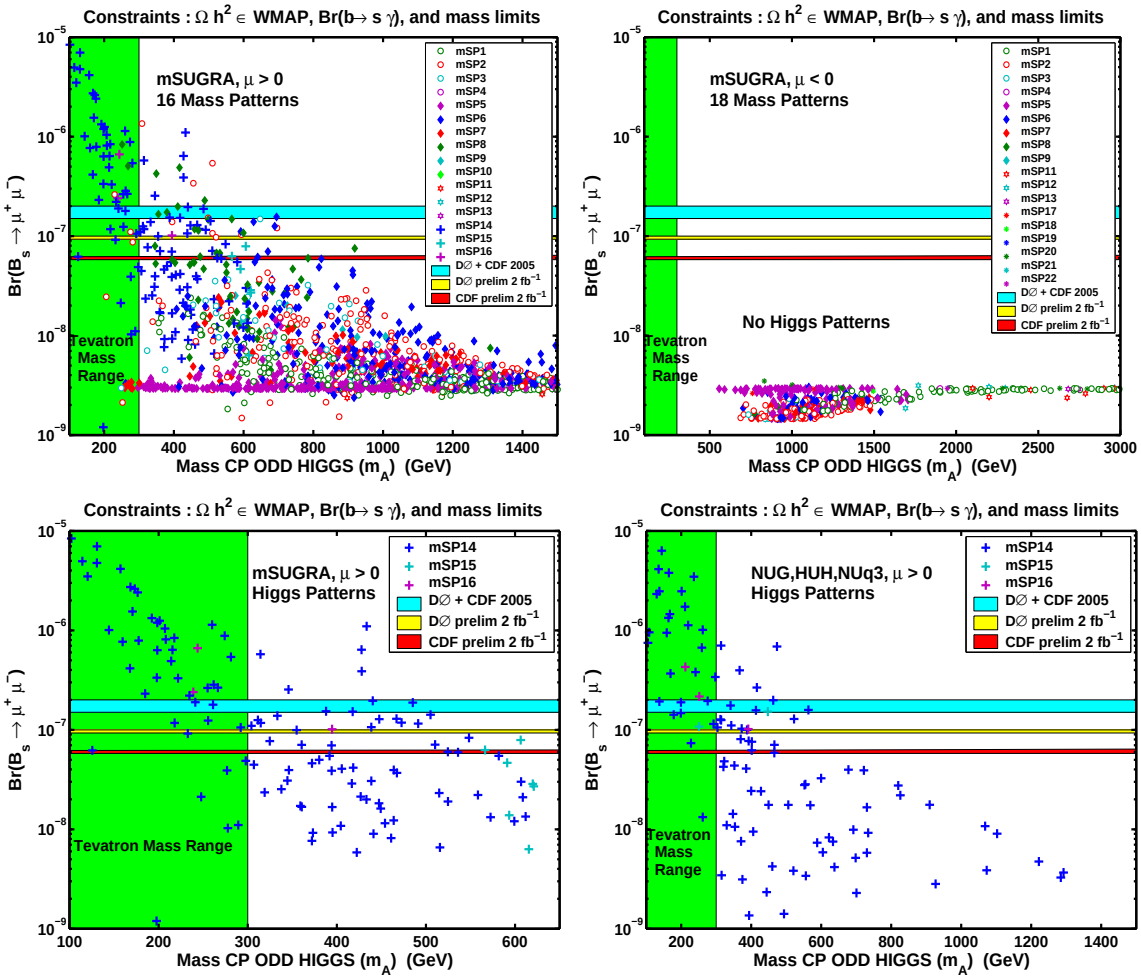

Figure 3: (Color Online) Predictions for the branching ratio $B_s \to \mu^+\mu^-$ in various patterns in the SUGRA landscape. Upper left panel: predictions are for the patterns for $\mu > 0$ in mSUGRA; upper right panel: predictions are for the patterns for $\mu < 0$ in mSUGRA; lower left panel: predictions for the Higgs Patterns alone for $\mu > 0$ in mSUGRA; lower right panel: predictions for NUSUGRA models NUH, NUq3, and NUG for $\mu > 0$. The experimental limits are: top band 2005 [32, 33], and the bottom two horizontal lines are preliminary limits from the CDF and DØ data [10]. For convenience we draw the limits extending past the observable mass of the CP odd Higgs at the Tevatron.

currently underway and improved experiments in the future [37, 38, 39, 40, 41, 42]. Indeed the analysis of Fig.(4) shows that some of the parameter space of the Higgs Patterns is beginning to be constrained by the CDMS and the Xenon10 data [41].

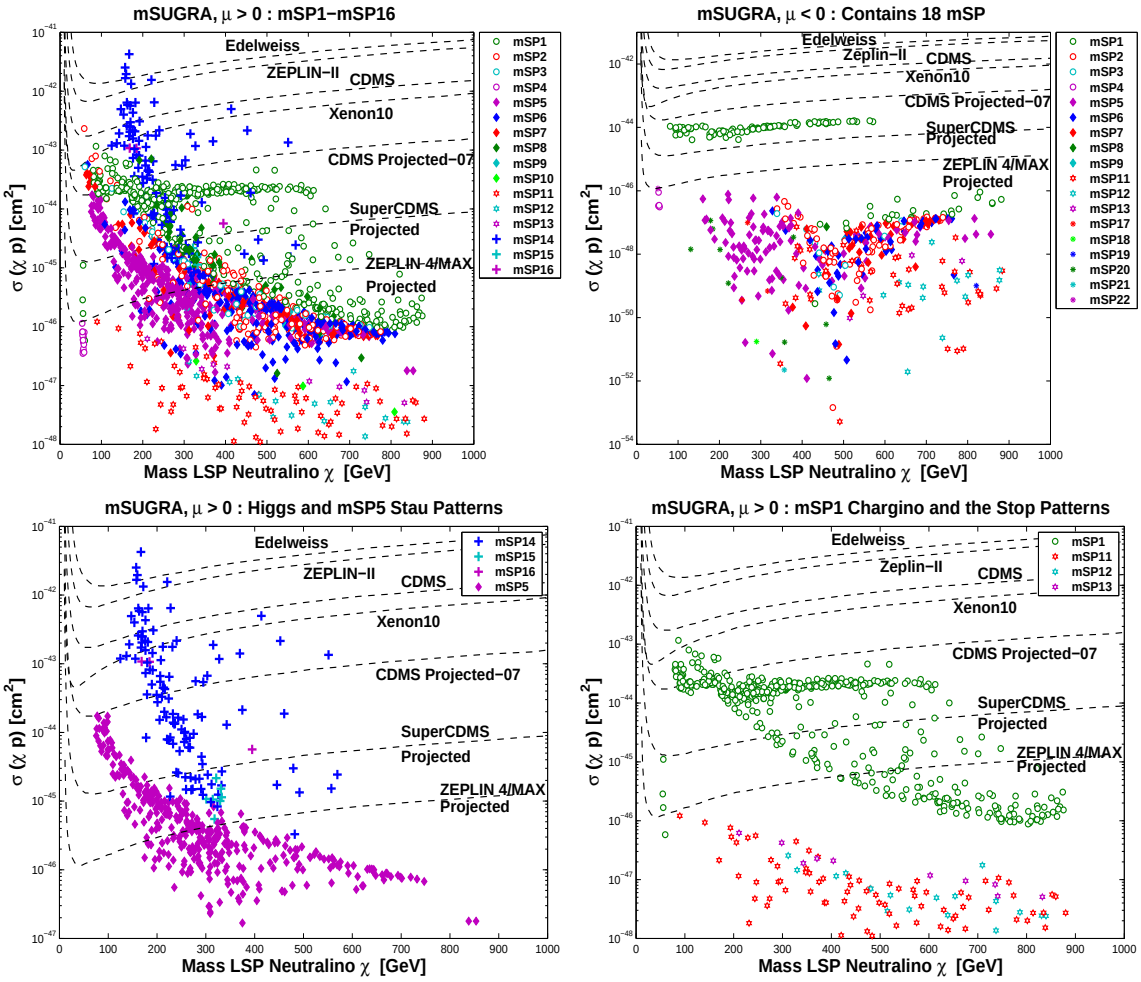

Figure 4: (Color Online) Analysis of $\sigma(\chi p)$ for mSUGRA: upper left panel: $\mu > 0$ case including all patterns; upper right panel: $\mu < 0$ allowing all patterns; lower left hand panel: A comparison of $\sigma(\chi p)$ for HPs and a stau NLSP case which is of type mSP5 for $\mu > 0$; lower right panel: a comparison of $\sigma(\chi p)$ for the Chargino Pattern mSP1 vs the Stop Patterns mSP11-mSP13. The analysis shows a Wall consisting of a clustering of points in the Chargino Patterns mSP1-mSP4 with a $\sigma(\chi p)$ in the range $10^{-44\pm.5}$ cm^2 enhancing the prospects for the observation of dark matter by SuperCDMS [43], ZEPLIN-MAX[44] or LUX[42] in this region.

What is very interesting is the fact that for the case $\mu > 0$ the $B_s \to \mu^+\mu^-$ limits, the Tevatron limits on the CP odd Higgs boson production, and the CDMS and Xenon10 limits converge on constraining the Higgs Patterns and specifically the pattern mSP14 and as well as some other patterns. Thus the CDMS and Xenon10 constraints on the mSPs are strikingly similar to the constraints of $B_s \to \mu^+\mu^-$ from the Tevatron. We also observe that although the case $\mu < 0$ is not currently accessible to the $B_s \to \mu^+\mu^-$ constraint (and may also be beyond the

ATLAS/CMS sensitivity for $B_s \to \mu^+\mu^-$), it would, however, still be accessible at least partially to dark matter experiment. Finally we remark that the proton-neutralino cross sections act as a discriminator of the SUGRA patterns as it creates a significant dispersion among some of the patterns (see upper left and the two lower panels in Fig.(4)).

Nonuniversalities of soft breaking: Since the nature of physics at the Planck scale is largely unknown it is useful to consider other soft breaking scenarios beyond mSUGRA. One such possibility is to consider nonuniveralities in the Kähler potential, which can give rise to nonuniversal soft breaking consistent with flavor changing neutral current constraints. We consider three possibilities which are nonuniversalities in (i) the Higgs sector (NUH), (ii) the third generation squark sector (NUq3), and (iii) the gaugino sector (NUG) (for a sample of previous work on dark matter analyses with nonuniversalities see [45]). We parametrize these at the GUT scale as follows: (i) NUH: $M_{H_u} = m_0(1+\delta_{H_u})$, $M_{H_d} = m_0(1+\delta_{H_d})$, (ii) NUq3: $M_{q3} = m_0(1+\delta_{q3})$, $M_{u3,d3} = m_0(1+\delta_{tbR})$, and, (iii) NUG: $M_1 = m_{1/2}$, $M_2 = m_{1/2}(1+\delta_{M_2})$, $M_3 = m_{1/2}(1+\delta_{M_3})$, with $-0.9 \leqslant \delta \leqslant 1$. In each case we carry out a Monte Carlo scan of 1×10^6 models. The above covers a very wide array of models. The analysis here shows that the patterns that appear in mSUGRA (i.e., mSPs) also appear here. However, in addition to the mSPs, new patterns appear which are labeled NUSP1-NUSP15 (see Table(2)), and we note the appearance of gluino patterns, and patterns where both the Higgses and gluinos are among the lightest sparticles. The neutral Higgs production cross section for the NUSUGRA case is given in the right panel of Fig.(2). The analysis shows that the Higgs Patterns produce the largest cross sections followed by the Chargino Patterns as in mSUGRA case. The constraints of $\mathcal{B}r(B_s \to \mu^+\mu^-)$ on the NUSUGRA Higgs patterns are exhibited in the lower right hand panel of Fig.(3). Again one finds that the $\mathcal{B}r(B_s \to \mu^+\mu^-)$ data constrains the parameter space of the HPs in the NUSUGRA case. One feature which is now different is that the Higgs Patterns survive significantly beyond the CP odd Higgs mass of 600 GeV within our assumed naturalness assumptions. Thus nonuniversalities tend to extend the CP odd Higgs beyond what one has in the mSUGRA case.

NUSP Label	Pattern	NUSP Label	Pattern
NUSP1	$\widetilde{\chi}_1^0 < \widetilde{\chi}_1^\pm < \widetilde{\chi}_2^0 < \widetilde{t}_1$	**NUSP2**	$\widetilde{\chi}_1^0 < \widetilde{\chi}_1^\pm < A, H$
NUSP3	$\widetilde{\chi}_1^0 < \widetilde{\chi}_1^\pm < \widetilde{\tau}_1 < \widetilde{\chi}_2^0$	**NUSP4**	$\widetilde{\chi}_1^0 < \widetilde{\chi}_1^\pm < \widetilde{\tau}_1 < \widetilde{l}_R$
NUSP5	$\widetilde{\chi}_1^0 < \widetilde{\tau}_1 < \widetilde{\nu}_\tau < \widetilde{\tau}_2$	**NUSP6**	$\widetilde{\chi}_1^0 < \widetilde{\tau}_1 < \widetilde{\nu}_\tau < \widetilde{\chi}_1^\pm$
NUSP7	$\widetilde{\chi}_1^0 < \widetilde{\tau}_1 < \widetilde{t}_1 < A, H$	**NUSP8**	$\widetilde{\chi}_1^0 < \widetilde{\tau}_1 < \widetilde{l}_R < \widetilde{\nu}_\mu$
NUSP9	$\widetilde{\chi}_1^0 < \widetilde{\tau}_1 < \widetilde{\chi}_1^\pm < \widetilde{l}_R$	**NUSP10**	$\widetilde{\chi}_1^0 < \widetilde{t}_1 < \widetilde{g} < \widetilde{\chi}_1^\pm$
NUSP11	$\widetilde{\chi}_1^0 < \widetilde{t}_1 < A, H$	**NUSP12**	$\widetilde{\chi}_1^0 < A, H < \widetilde{g}$
NUSP13	$\widetilde{\chi}_1^0 < \widetilde{g} < \widetilde{\chi}_1^\pm < \widetilde{\chi}_2^0$	**NUSP14**	$\widetilde{\chi}_1^0 < \widetilde{g} < \widetilde{t}_1 < \widetilde{\chi}_1^\pm$
NUSP15	$\widetilde{\chi}_1^0 < \widetilde{g} < A, H$		

Table 2: New 4 sparticle mass patterns for NUSUGRA in a 3×10^6 model scan of the parameter space with nonuniversalites. The new patterns are labeled NUSP1-NUSP15. NUSP(1,2,5,6) appear in NUq3 and NUSP(1,3,4;7-15) appear in NUG. NUH contains only mSPs.

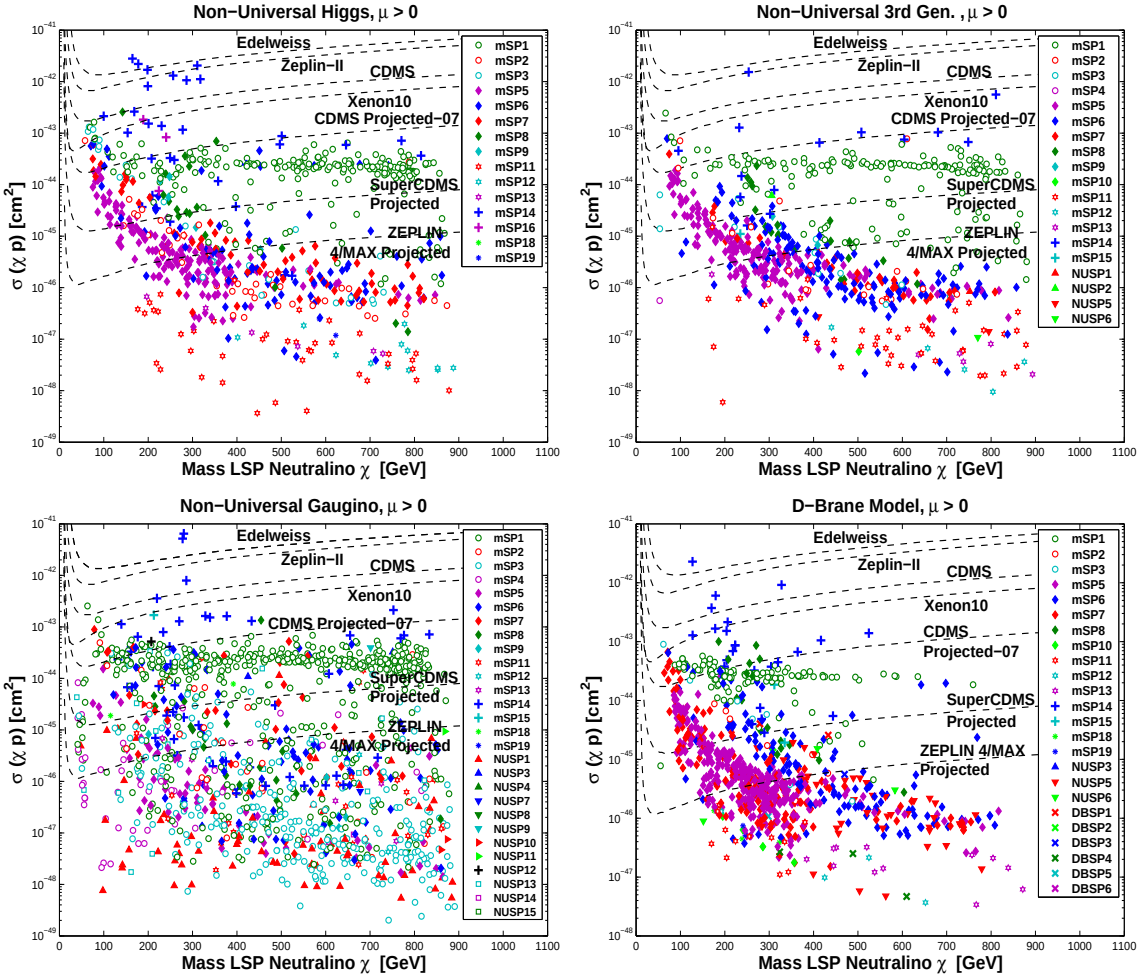

Figure 5: (Color Online) Analysis of the scalar cross section $\sigma(\chi p)$ for NUSUGRA and D-brane models: NUH (upper left panel), NUq3 (upper right panel), NUG (lower left panel), and brane models (lower right panel). As in Fig.(4) the Wall consisting of a clustering of points in the Chargino Patterns mSP1-mSP4 persists up to an LSP mass of about 900 GeV with a $\sigma(\chi p)$ in the range $10^{-44\pm.5}$ cm^2 enhancing the prospects for the observation of dark matter by SuperCDMS and ZEPLIN-MAX in this region.

Next we analyze the direct detection of dark matter in NUSUGRA. The results of the analysis are presented in Fig.(5) (upper two panels and the lower left panel). As in the mSUGRA case one finds that the largest dark matter cross sections still arise from the Higgs Patterns followed by the Chargino Patterns within the three types of nonuniversality models considered: NUH (upper left panel of Fig.(5)), NUq3 (upper right panel of Fig.(5)), NUG (lower left panel of Fig.(5)). Again the analysis within NUSUGRA shows the phenomenon of the Chargino Wall, i.e., the existence of a copious number of Chargino Patterns (specifically mSP1) in all cases with cross sections in the range $10^{-44\pm.5}\text{cm}^2$. Most of the parameter points along the Chargino Wall lie on the Hyperbolic Branch/Focus Point (HB/FP) region[46] where the Higgsino components of the LSP are substantial (for a review see [49]). Thus this Chargino Wall presents an encouraging region of the parameter space where the dark matter may become observable in improved experiments.

Light Higgses and Dark Matter in D-brane Models: The advent of D-branes has led to a new wave of model building [50], and several Standard Model like extensions have been constructed using intersecting D-branes [51]. The effective action and soft breaking in such models have been discussed [52] and there is some progress also on pursuing the phenomenology of intersecting D-brane models [53, 54, 55]. Here we discuss briefly the Higgses and dark matter in the context of D-branes. In our analysis we use the scenario of toroidal orbifold compactification based on $\mathcal{T}^6/\mathbb{Z}_2\times\mathbb{Z}_2$ where $\mathcal{T}^6$ is taken to be a product of 3 $\mathcal{T}^2$ tori. This model has a moduli sector consisting of volume moduli t_m, shape moduli u_m $(m=1,2,3)$ and the axion-dilaton field s. The detailed form of the soft breaking in D-brane models can be found in [52], and we focus here on the $\frac{1}{2}$ BPS sector. Specifically the parameter space consists of the gravitino mass $m_{3/2}$, the gaugino mass $m_{1/2}$, the trilinear coupling A_0, $\tan\beta$, the stack angle α $(0\leqslant\alpha\leqslant\frac{1}{2})$, the Goldstino angle [56] θ, the moduli VEVs, Θ_{t_i}, Θ_{u_i} $(i=1,2,3)$ obeying the sum rule $\sum_{i=1}^{3}F_i=1$, where $F_i=|\Theta_{t_i}|^2+|\Theta_{u_i}|^2$, and sign$(\mu)$ (see Appendix A of the first paper in [52] for details). In the analysis we ignore the exotics, set $F_3=0, 0\leqslant F_1\leqslant 1$, and use the naturalness assumptions similar to the mSUGRA case with $\mu>0$. The analysis shows that the allowed parameter space is dominated by the mSPs with only six new patterns (at isolated points) emerging. Specifically all the HPs (mSP14-mSP16) are seen to emerge in good abundance. Regarding the new patterns we label these patterns D-brane Sugra Patterns (DBSPs) since the patterns arise in the SUGRA field point limit of the D-branes. Specifically we find six new patterns DBSP$(1-6)$ as follows

$$\begin{array}{ll}
\text{DBSP1}: \widetilde{\chi}_1^0<\widetilde{\tau}_1<\widetilde{\nu}_\tau<A/H\ ; & \text{DBSP2}: \widetilde{\chi}_1^0<\widetilde{\tau}_1<\widetilde{\nu}_\tau<\widetilde{l}_R\ ; \\
\text{DBSP3}: \widetilde{\chi}_1^0<\widetilde{\tau}_1<\widetilde{\nu}_\tau<\widetilde{\nu}_\mu\ ; & \text{DBSP4}: \widetilde{\chi}_1^0<\widetilde{t}_1<\widetilde{\tau}_1<\widetilde{\nu}_\tau\ ; \\
\text{DBSP5}: \widetilde{\chi}_1^0<\widetilde{\nu}_\tau<\widetilde{\tau}_1<\widetilde{\nu}_\mu\ ; & \text{DBSP6}: \widetilde{\chi}_1^0<\widetilde{\nu}_\tau<\widetilde{\tau}_1<\widetilde{\chi}_1^\pm\ .
\end{array} \tag{3}$$

The analysis of the Higgs production cross section $\sigma_{\Phi\tau\tau}(pp)$ in the D-brane models at the LHC is given in the left panel of Fig.(6). The analysis shows that the HPs again dominate the Higgs production cross sections. One also finds that the $B_s\to\mu^+\mu^-$ experiment constraints the HPs in this model as seen in the right panel of Fig.(6). The dark matter scalar cross section $\sigma(\widetilde{\chi}_1^0 p)$

DBSPs	$m_{3/2}$ (GeV)	$m_{1/2}$ (GeV)	A_0 (GeV)	$\tan\beta$	α	$\cos^2\theta$	F_1
DBSP1	3654	1018	-331	51.5	0.444	0.705	0.086
DBSP4	1962	777	5863	9.4	0.430	0.790	0.260
DBSP5	2114	718	3512	21.3	0.448	0.688	0.051

Table 3: Benchmarks for D-brane models DBSPs.

is given in the lower right panel of Fig.(5). Here also one finds that the Higgs Patterns typically give the largest scalar cross sections followed by the Chargino Patterns (mSP1-mSP3) and then by the Stau Patterns. Further, one finds that the Wall of Chargino Patterns persists in this case as well.

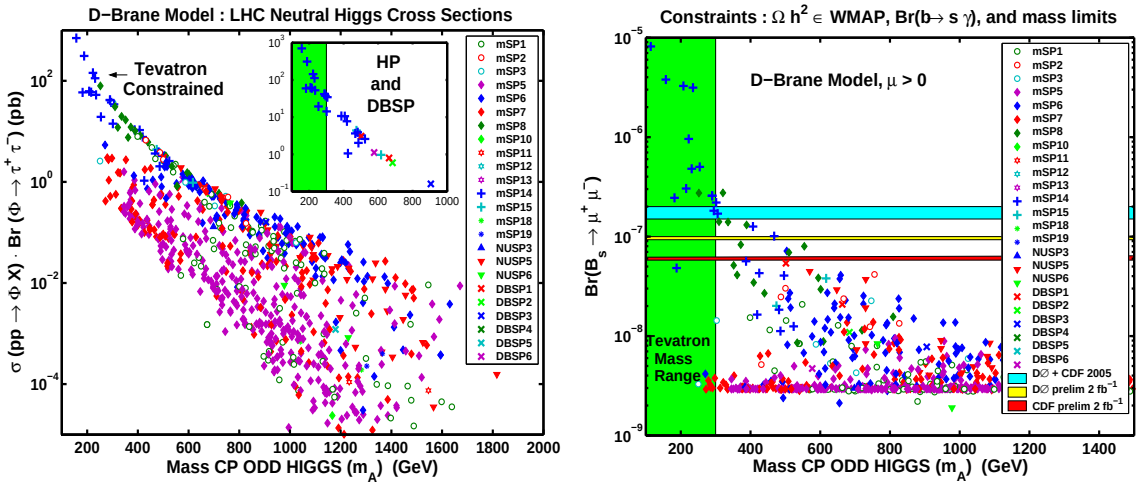

Figure 6: (Color Online) Predictions in D-brane models for $\mu > 0$: The Higgs production cross section $\sigma_{\Phi\tau\tau}(pp)$ at the LHC as a function of the CP odd Higgs mass m_A (left panel); $B_s \to \mu^+\mu^-$ vs m_A (right panel). The experimental constraints from the Tevatron are shown and constrain the Higgs Patterns.

We comment briefly on the signals from the chargino patterns. The chargino patterns correspond typically to low values of $m_{1/2}$ and arise dominantly from the hyperbolic branch/focus point region of radiative breaking of the electroweak symmetry. The above situation then gives rise to light charginos and neutralinos which can produce a copious number of leptonic signatures. We note that in the recent analysis of Ref.[1], the chargino pattern was studied in detail and the signatures at the LHC investigated. In particular it is found that the chargino patterns can give rise to substantial di-lepton and tri-leptonic signatures. Thus suppose we consider a model point in mSUGRA $\mu > 0$ that sits on the Chargino Wall with $(m_0, m_{1/2}, A_0, \tan\beta) = (885, 430, 662, 50.2)$ (mass units in GeV). Here $(m_{\widetilde{\chi}^0_1}, m_{\widetilde{\chi}^\pm_1}) \sim (177, 324)$ GeV with $\sigma(\widetilde{\chi}^0_1 p) \sim 1 \times 10^{-8}$ pb, and $\Omega_{\widetilde{\chi}^0_1} h^2 \sim .085$. An analysis of leptonic signatures at the LHC with 10 fb^{-1} in this case gives the number of di-lepton and tri-lepton SUSY events (N) with the cuts im-

posed as in Ref.[1], so that $(N_{2L}, N_{3L})_{jet\geq 2} \sim (350, 40)$, (where $(L = e, \mu)$). Both signatures are significantly above the 5σ discovery limits at the LHC (see Ref.[1]).

Conclusions: It is seen that Higgs Patterns (HPs) arise in a wide range of models: in mSUGRA, in NUSUGRA and in D-brane models. The HPs are typically seen to lead to large Higgs production cross sections at the Tevatron and at the LHC, and to the largest $B_s \to \mu^+\mu^-$ branching ratios, and thus are the first to be constrained by the $B_s \to \mu^+\mu^-$ experiment. It is also seen that the HPs lead typically to the largest neutralino-proton cross sections and would either be the first to be observed or the first to be constrained by dark matter experiment. The analysis presented here shows the existence of a Chargino Wall consisting of a copious number of parameter points in the Chargino Patterns where the NLSP is a chargino which give a $\sigma(\tilde{\chi}_1^0 p)$ at the level of $10^{-44\pm.5}\text{cm}^2$ in all models considered for the LSP mass extending up to 900 GeV in many cases. These results heighten the possibility for the observation of dark matter in improved dark matter experiments such as SuperCDMS[43], ZEPLIN-MAX[44], and LUX[42] which are expected to reach a sensitivity of 10^{-45} cm^2 or more. Finally, we note that several of the patterns are well separated in the $\sigma(\tilde{\chi}_1^0 p)$- LSP mass plots, providing important signatures along with the signatures from colliders for mapping out the sparticle parameter space.

Acknowledgements: This work is supported in part by NSF grant PHY-0456568.

References

[1] D. Feldman, Z. Liu and P. Nath, Phys. Rev. Lett. **99**, 251802 (2007)

[2] A. H. Chamseddine, R. Arnowitt and P. Nath, Phys. Rev. Lett. **49**, 970 (1982); P. Nath, R. Arnowitt and A. H. Chamseddine, Nucl. Phys. B **227**, 121 (1983).

[3] R. Barbieri, S. Ferrara and C.A. Savoy, Phys. Lett. **B119**, 343 (1982).

[4] L. Hall, J. Lykken and S. Weinberg, Phys. Rev. **D27**, 2359 (1983).

[5] A. Djouadi, M. Drees and J. L. Kneur, JHEP **0603**, 033 (2006); Phys. Lett. B **624** (2005) 60; U. Chattopadhyay, D. Das, A. Datta and S. Poddar, Phys. Rev. D **76** (2007) 055008; M. E. Gomez, T. Ibrahim, P. Nath and S. Skadhauge, Phys. Rev. D **72**, 095008 (2005); J. L. Feng, A. Rajaraman and B. T. Smith, Phys. Rev. D **74**, 015013 (2006); H. Baer, V. Barger, G. Shaughnessy, H. Summy and L. t. Wang, Phys. Rev. D **75** (2007) 095010; R. Arnowitt, A. Arusiano, B. Dutta, T. Kamon, N. Kolev, P. Simeon, D. Toback, and P. Wagner, Phys. Lett. B **649**, 73 (2007).

[6] D. N. Spergel *et al.*, astro-ph/0603449.

[7] E. Barberio *et al.*, HFAG Collaboration], arXiv:0704.3575 [hep-ex].

[8] M. Misiak *et al.*, Phys. Rev. Lett. **98** (2007) 022002.

[9] G. Degrassi, P. Gambino and G. F. Giudice, JHEP **0012** (2000) 009; A. J. Buras et.al., Nucl. Phys. B **659** (2003) 3; M. E. Gomez, T. Ibrahim, P. Nath and S. Skadhauge, Phys. Rev. D **74** (2006) 015015; G. Degrassi, P. Gambino and P. Slavich, Phys. Lett. B **635** (2006) 335.

[10] CDF Public Note 8956; DØ Conference Note 5344-CONF.

[11] R. Barate *et al.,* Phys. Lett. B **565**, 61 (2003); LHWG-Note 2005-01; G. Abbiendi *et al.* [OPAL Collaboration], arXiv:0707.0373 [hep-ex].

[12] G. Abbiendi *et al.* [OPAL Collaboration], Eur. Phys. J. C **35**, 1 (2004);

[13] G. Belanger, F. Boudjema, A. Pukhov and A. Semenov, [hep-ph/0607059]; Comput. Phys. Commun. **174**, 577 (2006).

[14] A. Djouadi, J. L. Kneur and G. Moultaka, Comput. Phys. Commun. **176**, 426 (2007).

[15] F. E. Paige, S. D. Protopopescu, H. Baer and X. Tata, arXiv:hep-ph/0312045.

[16] W. Porod, Comput. Phys. Commun. **153**, 275 (2003).

[17] B. C. Allanach, Comput. Phys. Commun. **143**, 305 (2002).

[18] H. Baer, J. Ferrandis, S. Kraml and W. Porod, Phys. Rev. D **73**, 015010 (2006).

[19] G. Belanger, S. Kraml and A. Pukhov, Phys. Rev. D **72**, 015003 (2005).

[20] B. C. Allanach, A. Djouadi, J. L. Kneur, W. Porod and P. Slavich, JHEP **0409**, 044 (2004).

[21] B. C. Allanach, S. Kraml and W. Porod, JHEP **0303**, 016 (2003).

[22] B. C. Allanach *et al.*, [arXiv:hep-ph/0202233].

[23] M. Battaglia, A. De Roeck, J. R. Ellis, F. Gianotti, K. A. Olive and L. Pape, Eur. Phys. J. C **33**, 273 (2004).

[24] T. C. Yuan, R. Arnowitt, A. H. Chamseddine and P. Nath, Z. Phys. C **26**, 407 (1984); D. A. Kosower, L. M. Krauss and N. Sakai, Phys. Lett. B **133**, 305 (1983); J.L. Lopez, D.V. Nanopoulos, X. Wang, Phys. Rev. **D49**, 366(1994); U. Chattopadhyay and P. Nath, Phys. Rev. D **53**, 1648 (1996); T. Ibrahim and P. Nath, Phys. Rev. D **61**, 095008 (2000).

[25] G. W. Bennett *et al.* [Muon g-2 Collaboration], Phys. Rev. Lett. **92** (2004) 161802.

[26] K. Hagiwara, A. D. Martin, D. Nomura and T. Teubner, Phys. Lett. B **649** (2007) 173.

[27] V. M. Abazov *et al.* [D0 Collaboration], Phys. Rev. Lett. **97**, 121802 (2006).

[28] G. L. Kane, B. D. Nelson, T. T. Wang and L. T. Wang, arXiv:hep-ph/0304134.

[29] M. S. Carena, D. Hooper and P. Skands, Phys. Rev. Lett. **97** (2006) 051801; M. S. Carena, D. Hooper and A. Vallinotto, Phys. Rev. D **75**, 055010 (2007).

[30] J. R. Ellis, S. Heinemeyer, K. A. Olive and G. Weiglein, Phys. Lett. B **653** (2007) 292.

[31] S. R. Choudhury and N. Gaur, Phys. Lett. B **451**, 86 (1999); K. S. Babu and C. Kolda, Phys. Rev. Lett. **84**, 228 (2000); A. Dedes, H. K. Dreiner, U. Nierste, and P. Richardson, Phys. Rev. Lett. **87**, 251804 (2001); R. Arnowitt, B. Dutta, T. Kamon and M. Tanaka, Phys. Lett. B **538** (2002) 121; S. Baek, P. Ko, and W. Y. Song, JHEP **0303**, 054 (2003); J. K. Mizukoshi, X. Tata and Y. Wang, Phys. Rev. D **66**, 115003 (2002); T. Ibrahim and P. Nath, Phys. Rev. D **67**, 016005 (2003).

[32] R. Bernhard *et al.* [CDF Collaboration], arXiv:hep-ex/0508058.

[33] A. Abulencia *et al.* [CDF Collaboration], Phys. Rev. Lett. **95** (2005) 221805.

[34] U. Chattopadhyay, T. Ibrahim and P. Nath, Phys. Rev. D **60** (1999) 063505.

[35] U. Chattopadhyay, A. Corsetti and P. Nath, Phys. Rev. D **68**, 035005 (2003) J. R. Ellis, K. A. Olive, Y. Santoso and V. C. Spanos, Phys. Lett. B **565**, 176 (2003); H. Baer, A. Belyaev, T. Krupovnickas and J. O'Farrill, JCAP **0408**, 005 (2004); J. Edsjo, M. Schelke, P. Ullio and P. Gondolo, JCAP **0304**, 001 (2003); P. Gondolo, J. Edsjo, P. Ullio, L. Bergstrom, M. Schelke and E. A. Baltz, JCAP **0407**, 008 (2004); Y. Mambrini and E. Nezri, [hep-ph/0507263]; M. M. Nojiri, G. Polesello and D. R. Tovey, JHEP **0603**, 063 (2006); D. Feldman, B. Kors and P. Nath, Phys. Rev. D **75**, 023503 (2007).

[36] S. Baek, D. G. Cerdeno, Y. G. Kim, P. Ko and C. Munoz, JHEP **0506** (2005) 017; D. G. Cerdeno and C. Munoz, JHEP **0410** (2004) 015; D. G. Cerdeno, T. Kobayashi and C. Munoz, arXiv:0709.0858 [hep-ph]; R. Arnowitt, B. Dutta and Y. Santoso, Nucl. Phys. B **606** (2001) 59.

[37] R. Bernabei *et al.*, Phys. Lett. B **389** (1996) 757.

[38] V. Sanglard *et al.* [The EDELWEISS Collaboration], Phys. Rev. D **71** (2005) 122002.

[39] D. S. Akerib *et al.* [CDMS Collaboration], Phys. Rev. Lett. **96** (2006) 011302.

[40] G. J. Alner *et al.*, Astropart. Phys. **28** (2007) 287; Astropart. Phys. **23** (2005) 444.

[41] J. Angle *et al.* [XENON Collaboration], arXiv:0706.0039 [astro-ph].

[42] T. Stiegler et.al., Fall Meeting of the Texas Sections of the APS and AAPT, 2007.

[43] R. W. Schnee *et al.* [The SuperCDMS Collaboration], arXiv:astro-ph/0502435.

[44] M. Atac *et al.*, New Astron. Rev. **49** (2005) 283.

[45] P. Nath and R. Arnowitt, Phys. Rev. D **56** (1997) 2820; A. Corsetti and P. Nath, Phys. Rev. D **64** (2001) 125010; J. R. Ellis, T. Falk, K. A. Olive and Y. Santoso, Nucl. Phys. B **652** (2003) 259; A. Birkedal-Hansen and B. D. Nelson, Phys. Rev. D **67** (2003) 095006; H. Baer, A. Mustafayev, S. Profumo, A. Belyaev and X. Tata, JHEP **0507** (2005) 065; G. Belanger, F. Boudjema, A. Cottrant, A. Pukhov and A. Semenov, Nucl. Phys. B **706** (2005) 411.

[46] K. L. Chan, U. Chattopadhyay and P. Nath, Phys. Rev. D **58**, 096004 (1998); J. L. Feng, K. T. Matchev and T. Moroi, Phys. Rev. Lett. **84**, 2322 (2000); H. Baer, C. Balazs, A. Belyaev, T. Krupovnickas and X. Tata, JHEP **0306**, 054 (2003).

[47] J. Campbell, R. K. Ellis, F. Maltoni and S. Willenbrock, Phys. Rev. D **67** (2003) 095002; R. V. Harlander and W. B. Kilgore, Phys. Rev. D **68**, 013001 (2003); F. Maltoni, Z. Sullivan and S. Willenbrock, Phys. Rev. D **67** (2003) 093005; S. Dawson, C. B. Jackson, L. Reina and D. Wackeroth, Mod. Phys. Lett. A **21** (2006) 89; U. Aglietti *et al.*, arXiv:hep-ph/0612172.

[48] CDF Public Note 8594 v1.0; A. Anastassov, Aspen 2008 Winter Conference: "Revealing the Nature of Electroweak Symmetry Breaking".

[49] A. B. Lahanas, N. E. Mavromatos and D. V. Nanopoulos, Int. J. Mod. Phys. D **12** (2003) 1529.

[50] R. Blumenhagen, M. Cvetic, P. Langacker and G. Shiu, Ann. Rev. Nucl. Part. Sci. **55** (2005) 71; R. Blumenhagen, B. Kors, D. Lust and S. Stieberger, Phys. Rept. **445** (2007) 1.

[51] R. Blumenhagen, B. Körs, D. Lüst and T. Ott, Nucl. Phys. B **616** (2001) 3; M. Cvetic, G. Shiu and A. M. Uranga, Phys. Rev. Lett. **87** (2001) 201801 Nucl. Phys. B **615** (2001) 3; D. Cremades, L. E. Ibanez and F. Marchesano, Nucl. Phys. B **643** (2002) 93; C. Kokorelis, JHEP **0209** (2002) 029; G. Honecker and T. Ott, Phys. Rev. D **70** (2004) 126010; C. M. Chen, T. Li, V. E. Mayes and D. V. Nanopoulos, arXiv:0711.0396 [hep-ph].

[52] B. Kors and P. Nath, Nucl. Phys. B **681** (2004) 77; D. Lust, S. Reffert and S. Stieberger, Nucl. Phys. B **706** (2005) 3; T. W. Grimm and J. Louis, Nucl. Phys. B **699** (2004) 387.

[53] F. Quevedo, http:/ /www. slac. stanford. edu/spires/ find/hep/ www?irn=5772753.

[54] G. L. Kane, P. Kumar, J. D. Lykken and T. T. Wang, Phys. Rev. D **71** (2005) 115017.

[55] M. Cvetic, P. Langacker and G. Shiu, Phys. Rev. D **66** (2002) 066004.

[56] A. Brignole, L. E. Ibanez and C. Munoz, arXiv:hep-ph/9707209.